



## Kinetic, isotherm, and thermodynamic studies of polycyclic aromatic hydrocarbons biosorption from petroleum refinery wastewater using spent waste biomass

Sherif A. Younis, Nour Sh. El-Gendy\*, Waleed I. El-Azab, Yasser M. Moustafa

Egyptian Petroleum Research Institute, P.O. 11727, 1 Ahmed El-Zomor St., El-Zohour Region, Nasr City, Cairo, Egypt, emails: [sherifali\\_r@yahoo.com](mailto:sherifali_r@yahoo.com) (Sh.A. Younis), [nourepri@yahoo.com](mailto:nourepri@yahoo.com) (N.Sh. El-Gendy), [welazab@yahoo.com](mailto:welazab@yahoo.com) (W.I. El-Azab), [ymoustafa12@yahoo.com](mailto:ymoustafa12@yahoo.com) (Y.M. Moustafa)

Received 29 March 2014; Accepted 5 September 2014

### ABSTRACT

Removal of polycyclic aromatic hydrocarbons (PAHs) from petroleum refinery wastewater was investigated using spent waste biomass [rice straw (RS) and sugarcane bagasse (SB)] from bioethanol production process as low-cost biosorbents of natural origin. The equilibrium sorption capacity has been significantly improved by increasing the initial PAHs concentration, contact time, and temperature. The biosorption equilibrium of PAHs onto SB and RS was achieved in approximately 180 min with uptake capacity of the three PAHs followed the order: SB > RS at all studied initial concentrations ( $q_e$  approximately recorded 3.61, 1.01, and 0.86 mg/g SB and 3.35, 0.77, and 0.73 mg/g RS at initial concentrations of 150, 50, and 50 mg/L for naphthalene, anthracene, and pyrene, respectively). The sorption kinetics data best fitted the pseudo-first-order rate model for naphthalene, and the pseudo-second-order rate model for anthracene and pyrene. The adsorption isotherms of PAHs were in agreement well with Langmuir isotherm model for all three PAHs molecules at different temperatures than Freundlich and Temkin isotherm models, and the adsorption mechanism was dominated by a combination of physical and chemical adsorption. Thermodynamic parameters suggested that the sorption of the three PAHs onto both SB and RS is endothermic and nonspontaneous.

**Keywords:** Petroleum refinery wastewater; Polycyclic aromatic hydrocarbons; Biosorption; Kinetic study; Equilibrium isotherm; Thermodynamic analyses

### 1. Introduction

The conventional treatment configuration of petroleum refinery wastewater (PRWW) is not suitable to remove light fraction of aliphatic and aromatic petroleum hydrocarbons and chlorinated organic substances originated from the cooling liquids used in refineries,

resulting in subsequent disposal problem of these contaminants to receiving water bodies. So, there is still a need for cost-effective and highly efficient treatment techniques to remove the remaining toxic aromatic pollutants found in PRWW.

Polycyclic aromatic hydrocarbons (PAHs) as typical persistent organic pollutants are priority pollutants of most concern due to their high bioaccumulation, carcinogenic, mutagenic, and toxic properties [1,2].

\*Corresponding author.

PAHs are often resistant and difficult to be removed by conventional physicochemical treatment methods [3,4]. However, adsorption is one of the most economical and effective techniques for removing organic pollutants at low concentration. Activated carbon is the most widely used as a conventional adsorbent [3,5]. However, high cost and difficult regeneration limit its application in large-scale wastewater treatment [6].

In the last decade, extensive research has been undertaken to develop alternative and economic adsorbents. An economic adsorbent is defined as the one which is abundant in nature, or is a byproduct or waste from industry and requires little processing. Recently, different types of biosorbents, including algae, bacteria, yeasts, fungi, industrial wastes, agricultural wastes, and natural residues, are potential alternatives of conventional adsorbents owing to their inherent sorption capability, environmental compatibility, and cost-effectiveness [7–10]. Therefore, biosorption is considered an interesting alternative technology to remove organic pollutants from aqueous solutions.

The purpose of this study was to investigate the adsorption features of spent waste biomass; rice straw (RS) and sugarcane bagasse (SB) were obtained after bioethanol production without any pre-treatment as low-cost adsorbents to remove high concentrations of PAHs from PRWW. The effect of time, initial PAHs concentration, the sorption kinetic, equilibrium, and thermodynamic parameters at various temperatures were investigated.

## 2. Materials and methods

### 2.1. Chemicals and reagents

In the adsorption experiments, analytical standard naphthalene (Nap), anthracene (Ant), pyrene (Pyr) (Sigma Aldrich, St. Louis, MO, USA), high-performance liquid chromatography (HPLC)-grade acetonitrile, and distilled water Milli-Q were used. All other chemical reagents employed in this study were of analytical grade.

### 2.2. Biosorbents

Spent biomass of RS and SB was used in this study. They are waste byproducts of bioethanol production process undertaken in the Petroleum Biotechnology Laboratory of the Egyptian Petroleum Research Institute (1 Ahmed El-Zomor St., El-Zohour Region, Nasr City, Cairo, Egypt). The collected biomaterials were washed with hot deionized water, dried in a hot air

oven at 105°C until a constant weight, crushed with grinder, sieved to constant sizes (0.25–0.315 mm), and then used as it is without any further chemical or physical treatments.

### 2.3. Authentic PRWW preparation

In order to simulate the real feed of PRWW effluents, the authentic wastewater solution used in this work was prepared according to the physicochemical characteristics of petroleum refinery effluents collected from wastewater treatment plant at Cairo Oil Refining Company (Sharekat El Petrol St., Mostorod, Kalyobiya—Egypt) at different dates and time intervals (data not shown).

Stock solutions for each of the three PAHs (namely, naphthalene, anthracene and pyrene) 1,000 mg/L were prepared in acetone which were further diluted by authentic wastewater solution mixed with 30% (v/v) acetone. The utilization of acetone as a co-solvent was efficient for the solubilization of the PAHs in aqueous medium, in the concentration range used in this study and hamper adsorption at the walls of the flasks.  $\text{NaN}_3$ , 200 mg/L was added to inhibit the degradation by incidental bacteria as recommended by Chen et al. [2].

### 2.4. Batch biosorption experiments

A 100 mL glass Erlenmeyer flask sealed with PARAFILM “M” to prevent evaporative loss and an orbital shaker device set to operate at 150 rpm were used in the experiments. There was no considerable adsorption of analytes on the walls of the flasks, which was verified by comparing the PAHs concentrations in reaction mixtures with and without the adsorbent. All the batch biosorption experiments were conducted by contacting 25 mL of authentic wastewater solution of known concentration of each of the PAHs as single-component system (adsorbate) with 0.5 g of biosorbent. Biosorption capacity and percentage removal of the three PAHs were determined at different contact times with different initial concentrations to know the equilibrium contact time, and also the effect of temperature was studied. Table 1 illustrates all the process factors. Biosorbent was separated from the solution at predetermined time intervals by centrifugation at 4,000 rpm for 10 min, and the remaining concentrations of the studied three PAHs were determined by (HPLC) after three times extraction with 10 mL ethyl acetate.

Table 1

Different process conditions used for biosorption of the three PAHs (naphthalene, anthracene, and pyrene)

Process factors	Other conditions
Contact time (0–720 min)	Temperature: 303 K; biosorbent dosage: 2% w/v; initial pH $7 \pm 0.2$ ; different concentrations 10, 25, and 50 mg/L for anthracene and pyrene and 50, 75, and 150 mg/L for naphthalene.
Different temperatures 288, 303, and 318 K	Contact time: 300 min; biosorbent dosage: 2% w/v; initial pH $7 \pm 0.2$ ; different initial concentrations range from 10 to 150 mg/L for naphthalene and 2.5–50 mg/L for anthracene and pyrene.

### 2.5. PAHs analysis

HPLC instrument model Agilent 1200 series (Hewlett-Packard-Strasse 8, 76337 Waldbronn, Germany) equipped with auto sampler and photodiode array detector (set at full scan range 190–400 nm) was used to analyze Nap, Ant, and Pyr concentrations under the following condition; C8 reversed phase (4.6 X 25 cm, 300 Å, 5 µm) column, isocratic program with 60% acetonitrile: 40% water (v/v), flow rate 1.0 mL/min, and sample size 2 µL. The removal percentage and biosorption capacity ( $q_t$ ) mg/g were calculated as follows:

$$\text{Removal \%} = \frac{(C_o - C_t)}{C_o} \times 100 \quad (1)$$

$$q_t = \frac{(C_o - C_t)V}{M} \quad (2)$$

where  $C_o$  and  $C_t$  are the initial and final concentrations of the solute in the solution (mg/L), respectively,  $V$  (L) is the volume of the solution, and  $M$  (g) is the mass of the biosorbent. All the listed data were the arithmetic average of the obtained results from triplicate experiments to check reproducibility, and the margin errors for  $q_{exp}$  were  $\approx 3.2$ – $4.3\%$ ,  $2.8$ – $3.9\%$ , and  $2.1$ – $3.5\%$  and standard deviation of  $\approx 0.007$ ,  $0.05$ , and  $0.033$  mg/g for Nap, Ant, and Pyr, respectively, at a confidence level of 95%.

## 3. Results and discussion

### 3.1. Pre-equilibrium kinetics of different PAHs concentrations

The feasibility and efficiency of biosorption process depends not only on the properties of the adsorbate and biosorbent, but also on the initial adsorbate concentration in solution which might have implications on the adsorbent/adsorbate interactions [11,12]. The rate of biosorption and equilibrium time for PAHs uptake at 50–150 mg/L Nap (di-aromatic ring) and 10–50 mg/L Ant and Pyr (tri and four

aromatic rings, respectively) in single-pollutant system on the surface of SB and RS biosorbents as a function of time were studied and presented in (Fig. 1). The adsorption curves (Fig. 1) were smooth and continuous for all the studied PAHs leading to saturation on the outer interface of the SB and RS sorbents biomass and the possibility of monolayer coverage of PAHs [13,14].

It can be noted that, within 720 min of contact between PAHs and the biomass adsorbents (SB and RS), the adsorption process tends to reach the equilibrium state nearly after 90 min (Fig. 1). Therefore, equilibrium time was set conservatively at 180 min for further experiments to be sure that the equilibrium state was obtained. PAHs uptake increased with the initial increase in PAHs concentrations and was nearly recorded at 180 min; 2.12, 2.39, and 3.61 mg/g for SB and 2.04, 2.23, and 3.35 mg/g for RS at initial Nap concentration of 50, 75, and 150 mg/L, respectively; 0.29, 0.67, and 1.01 mg/g for SB and 0.25, 0.57, and 0.77 mg/g for RS at initial Ant concentration of 10, 25, and 50 mg/L, respectively, and 0.25, 0.61, and 0.61 mg/g for SB and 0.22, 0.51, and 0.73 mg/g for RS at initial Pyr concentration of 10, 25, and 50 mg/L, respectively. The increase in adsorption might be due to the increase in the driving force and mass transfer of PAHs molecules from the solution onto the biosorbent surface that results in higher adsorbate adsorption capacity ( $q_e$ , mg/g) [15,16]. Similar observations were reported by Agarry and Aremu [12] using orange peels for the removal of PAH from wastewater.

Furthermore, the results obtained in (Fig. 1) revealed that SB has higher affinity with higher adsorption capacity ( $q_t$ , mg/g) towards PAHs molecules than RS. This might be due to the high hydrophilic properties (Si concentrations) of RS relative to SB as confirmed by FTIR and EDX (data not shown). Also, the adsorption capacity and percentage removal of all the studied PAHs can be ranked in the following decreasing order; Nap > Ant > Pyr over all the studied concentrations. This order is consistent with the trend in molecular weight and molecular size that suggests a diffusive mass transfer-controlled process.

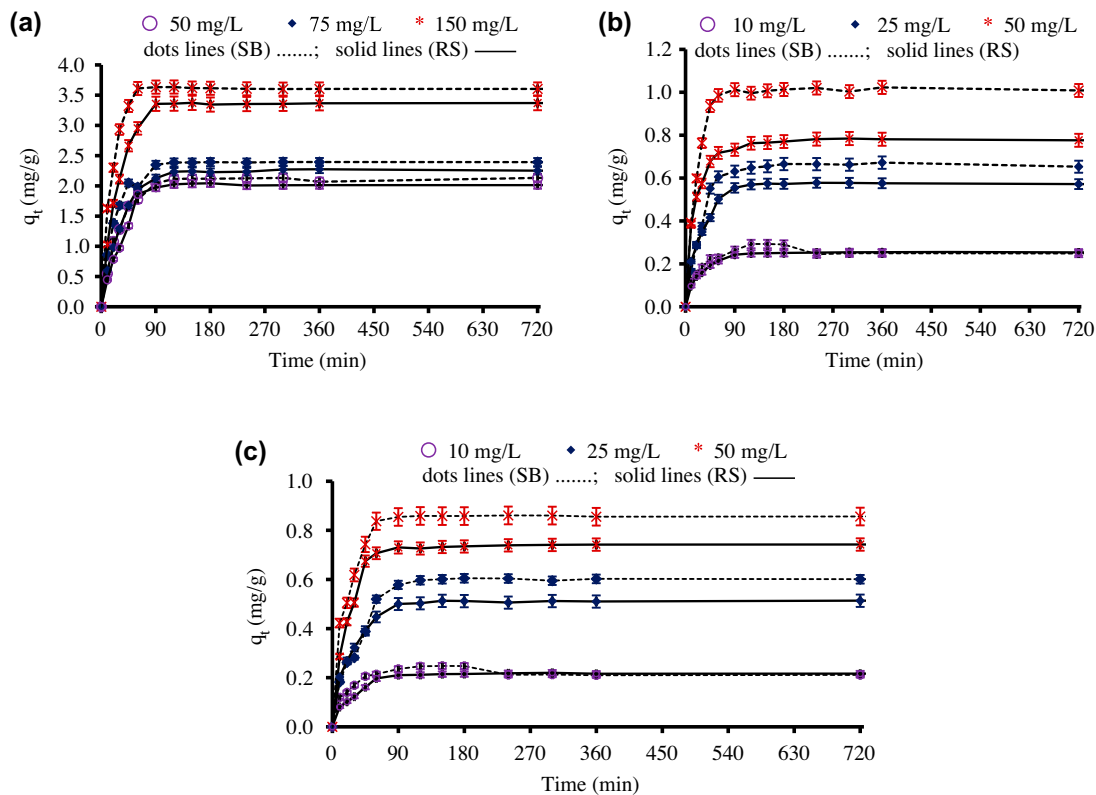


Fig. 1. Equilibrium time and adsorption capacity for (a) naphthalene, (b) anthracene, and (c) pyrene at different concentrations onto spent waste biomass of SB and RS from authentic wastewater solution (30% v/v acetone).

For a diffusion-controlled process, the rate of uptake should increase with the concentration gradient—the driving force for diffusion and, therefore, increase with the initial concentration that agrees with the experimental data obtained in this study. Based on these results, it can be suggested that the adsorption of PAHs onto the RS and SB surface appears to be controlled not only by hydrophobicity, but depends on number of factors including the nature of the adsorbent (its pore structure, functional groups) and the nature of the adsorbate that play an important role in determining the interactions between adsorbates and adsorbents. Mackay and Gschwend [17] and Yang et al. [18] have reported similar observations on the adsorption of PAHs onto single-walled and multi-walled carbon nanotubes.

### 3.2. Biosorption kinetic modeling

The results showed that adsorption of all PAHs appeared to have similar behavior (Fig. 1). Therefore, kinetic modeling of the experimental data was studied to find out the potential rate-controlling steps for

biosorption of PAHs onto the SB and RS, as well as, the mechanisms involved in the sorption process. Two kinetic models were used, namely pseudo-first-order Lagergren (Eq. (3)) and pseudo-second-order (Eq. (4)) rate models [19].

$$\log(q_e - q_t) = \log q_e - \frac{K_1}{2.303} t \quad (3)$$

$$\frac{t}{q_t} = \frac{1}{K_2 q_e^2} + \frac{1}{q_e} t \quad (4)$$

where  $q_e$  and  $q_t$  (mg/g) are the amounts of PAHs adsorbed at equilibrium and time  $t$  (min), respectively.  $K_1$  ( $\text{min}^{-1}$ ) and  $K_2$  ( $\text{g}/\text{mg min}$ ) are the rate constants in the pseudo-first and pseudo-second-order kinetic models, respectively.

A normalized deviation analysis ( $\Delta q_e\%$ ) represented by Eq. (5) [5] was examined for each experimental data-set. The lowest values of the  $\Delta q_e\%$  and highest correlation coefficients  $R^2$  were used for the

statistical evaluation of how well the experimental data fitted to each kinetic model.

$$\Delta q_t\% = \frac{\sum_{i=1}^N \left( \frac{q_{t,exp} - q_{t,calc}}{q_{t,exp}} \right)}{N} \times 100 \quad (5)$$

where  $q_{t,exp}$  and  $q_{t,calc}$  are the experimental and calculated adsorption capacities (mg/g), respectively, and  $N$  is the number of data points.

In this work, it was found that the pseudo-first-order model was best representing the kinetic data for Nap, while the pseudo-second-order model was best representing the kinetic data for biosorption of Ant and Pyr onto both SB and RS biomass sorbents and could be used to determine the equilibrium sorption capacity, rate constants, and percentage of removal. According to Chen et al. [2] and Ho and McKay [20], the pseudo-second-order model may be related to the occurrence of chemical or combination of both physical and chemical sorption processes, which may control the adsorption rate. This suggests that the overall rate of PAHs biosorption process appears to be controlled by both physical and chemical sorption processes, which involves the mass transfer of PAHs molecules from the liquid phase to the SB and RS adsorbents surface. Physical adsorption may be caused by the aromatic nature of PAHs, probably combined with Van der Waals strength or hydrophobic ( $\pi$ - $\pi$  dispersive) interaction and the electron donor-acceptor mechanism that involves carbonyl groups that predominate in RS and SB surface. Moreover, the hydrophobic sites available, lignin, on the RS and SB adsorbent matrices can be used more rapidly by most of the PAHs [21]. Ho [22] and Younis et al. [13] reported that chemical sorption can occur by the polar functional groups of lignin, which include alcohols,

aldehydes, ketones, acids, and ethers as chemical bonding agents. Also, the obtained results show the higher rate constants for the biosorption of PAHs onto SB relative to RS and its increment with the increase of the initial PAHs concentrations. These confirm that the initial concentration plays an important role in the sorption of PAHs on SB and RS sorbents biomass, and the adsorption mechanism includes polarity-dependent mechanism.

In this study, the experimental and theoretical maximum sorption capacities for the three PAHs onto SB and RS (Tables 2 and 3) were higher than those reported by other researchers. Crisafulli et al. [3] reported the maximum adsorption capacity for the four PAHs (naphthalene, acenaphthene, anthracene, and pyrene), expressed in mg/g, were as follows: 0.345 for sugar cane bagasse, 0.553 for green coconut shells, and 0.215 for chitin. Chen et al. [2] reported, 1.1 and 1.4 mg/g for phenanthrene biosorption on orange peel and wood chip, respectively.

### 3.3. Biosorption isotherm

Study of adsorption equilibrium isotherms is an important step in investigating adsorption processes, since it makes it possible to identify the relationship between the amounts of analyte adsorbed and in solution, after equilibrium is reached and provide fundamental physicochemical data for evaluating the applicability of the sorption process to design a unit operation [19]. Three models namely, Langmuir [23], Freundlich [24], and Temkin [25] isotherm models in their linear form are used in this study for a better understanding of the interactions between RS or SB adsorbents and PAHs. Equilibrium isotherm constants and the correlation coefficient,  $R^2$ , with  $\Delta q_e\%$  are listed in Tables 4 and 5.

Table 2

Parameters of kinetic models of adsorption pseudo-first-order and pseudo-second-order models at different initial PAHs concentrations by spent biomass SB

PAHs	$C_o$ (mg/L)	$q_e$ (mg/g)	Pseudo-first-order				Pseudo-second-order			
			$q_c$ (mg/g)	$K_1$ ( $\text{min}^{-1}$ )	$R^2$	$\Delta q_e$ (%)	$q_c$ (mg/g)	$K_2$ (g/mg min)	$R^2$	$\Delta q_e$ (%)
Naphthalene	50	2.15	2.15	0.034	0.99	2.69	2.17	0.037	0.99	10.31
	75	2.40	2.39	0.042	1.00	1.51	2.42	0.056	1.00	9.14
	150	3.64	3.64	0.055	1.00	1.45	3.64	0.065	1.00	7.75
Anthracene	10	0.29	0.27	0.032	0.99	9.82	0.27	0.335	0.99	7.35
	25	0.67	0.73	0.04	0.95	16.26	0.66	0.197	1.00	11.63
	50	1.02	1.13	0.058	0.98	14.31	1.02	0.166	0.99	9.75
Pyrene	10	0.25	0.22	0.037	0.97	10.77	0.23	0.553	0.99	7.59
	25	0.60	0.56	0.021	0.96	13.31	0.61	0.237	0.99	10.05
	50	0.86	0.79	0.042	0.98	11.00	0.86	0.122	0.99	8.01

Table 3

Parameters of kinetic models of adsorption pseudo-first-order and pseudo-second-order models at different initial PAHs concentrations by spent biomass RS

PAHs	$C_o$ (mg/L)	$q_e$ (mg/g)	Pseudo-first-order kinetic model				Pseudo-second-order kinetic models			
			$q_c$ (mg/g)	$K_1$ (min <sup>-1</sup> )	$R^2$	$\Delta q_e$ (%)	$q_c$ (mg/g)	$K_2$ (g/mg min)	$R^2$	$\Delta q_e$ (%)
Naphthalene	50	2.06	2.05	0.023	0.99	4.23	2.07	0.032	0.99	16.62
	75	2.28	2.29	0.029	1.00	1.73	2.26	0.045	0.99	14.54
	150	3.37	3.35	0.034	1.00	1.65	3.39	0.037	0.98	12.45
Anthracene	10	0.26	0.23	0.03	0.97	12.96	0.25	0.474	0.99	9.11
	25	0.58	0.53	0.027	0.98	13.32	0.58	0.229	1.00	10.37
	50	0.78	0.69	0.042	0.98	13.37	0.78	0.212	1.00	5.31
Pyrene	10	0.22	0.21	0.027	0.97	10.00	0.22	0.401	0.99	9.28
	25	0.51	0.47	0.03	0.98	12.94	0.51	0.282	0.99	9.67
	50	0.74	0.81	0.05	0.96	10.73	0.75	0.205	1.00	8.92

Table 4

Isotherm constants of Langmuir, Freundlich, and Temkin isotherm models at different temperatures for SB biosorption process

PAHs	Temp. (K)	$q_{e, max}$ (mg/g)	Langmuir isotherm				Freundlich isotherm				Temkin isotherm				
			$a_L$	$K_L$	$R^2$	$\Delta q_e$ (%)	$n$	$K_f$	$R^2$	$\Delta q_e$ (%)	$K_t$	$B$	$b$ (J/mol)	$R^2$	$\Delta q_e$ (%)
Naphthalene	288	3.31	0.016	0.101	0.99	4.62	1.47	0.19	0.99	8.09	0.17	1.30	1,838	0.99	6.95
	303	3.56	0.028	0.154	0.99	3.00	1.66	0.30	0.98	6.21	0.26	1.24	2,028	0.99	14.93
	318	3.73	0.045	0.233	0.99	4.59	1.83	0.43	0.96	9.18	0.39	1.21	2,182	0.98	14.32
Anthracene	288	0.74	0.068	0.075	0.99	3.72	1.57	0.10	0.97	10.68	0.70	0.24	10,164	0.99	15.52
	303	0.92	0.071	0.104	0.98	3.96	1.49	0.12	0.97	9.44	0.75	0.31	8,146	0.98	24.17
	318	1.13	0.077	0.145	0.97	6.54	1.41	0.16	0.96	9.17	0.89	0.38	6,920	0.98	35.17
Pyrene	288	0.73	0.057	0.066	0.99	4.12	1.51	0.08	0.97	10.47	0.62	0.24	10,028	0.99	18.79
	303	0.85	0.061	0.084	0.98	4.86	1.46	0.10	0.97	11.10	0.66	0.29	8,709	0.98	22.10
	318	1.02	0.089	0.140	0.98	5.12	1.50	0.15	0.96	8.75	0.94	0.34	7,877	0.98	28.85

Table 5

Isotherm constants of Langmuir, Freundlich, and Temkin isotherm models at different temperatures for RS biosorption process

PAHs	Temp. (K)	$q_{e, max}$ (mg/g)	Langmuir isotherm				Freundlich isotherm				Temkin isotherm				
			$a_L$	$K_L$	$R^2$	$\Delta q_e$ (%)	$n$	$K_f$	$R^2$	$\Delta q_e$ (%)	$K_t$	$B$	$b$ (J/mol)	$R^2$	$\Delta q_e$ (%)
Naphthalene	288	3.06	0.013	0.079	0.99	3.22	1.43	0.15	0.99	3.84	0.15	1.20	1,991	0.99	20.12
	303	3.32	0.025	0.129	0.99	3.70	1.69	0.28	0.99	4.51	0.23	1.16	2,169	0.98	14.94
	318	3.58	0.033	0.174	0.99	3.52	1.76	0.35	0.97	7.45	0.29	1.22	2,162	0.98	12.88
Anthracene	288	0.61	0.046	0.046	0.99	1.70	1.47	0.065	0.98	6.62	0.52	0.20	11,743	0.98	22.41
	303	0.77	0.054	0.069	0.97	4.77	1.43	0.084	0.97	10.66	0.60	0.27	9,478	0.98	22.92
	318	0.84	0.059	0.082	0.98	3.38	1.43	0.10	0.97	9.39	0.66	0.29	9,261	0.98	24.78
Pyrene	288	0.63	0.041	0.046	0.98	10.42	1.40	0.061	0.98	16.82	0.48	0.22	10,845	0.99	18.64
	303	0.74	0.047	0.061	0.98	6.80	1.41	0.078	0.98	12.55	0.53	0.26	9,525	0.99	20.95
	318	0.89	0.041	0.069	0.98	2.52	1.34	0.084	0.98	7.28	0.56	0.31	8,635	0.97	30.36

Langmuir sorption model is based on the assumption that the maximum sorption corresponds to a saturated monolayer of the molecules on the adsorbent

surface, with no lateral interaction between sorbed molecules [14]. The linear form of Langmuir equation (Eq. (6)) for homogenous surface is:

$$\frac{C_e}{q_e} = \frac{1}{K_L} + \frac{a_L}{K_L} C_e \quad (6)$$

where  $C_e$  is the concentration of PAHs at equilibrium (mg/L),  $q_e$  is the adsorption capacity at equilibrium (mg/g), and  $a_L$  (L/mg) and  $K_L$  (L/g) are the Langmuir isotherm constants.

In this work, the relatively lower values of Langmuir constant “ $a_L$ ” (< 0.3 L/g) [5] implies low surface energy of RS and SB biomass. This might indicate the occurrence of a probable strong bonding of the three PAHs molecules with the spent waste RS and SB biosorbents [26].

Freundlich isotherm model is an empirical expression that encompasses the heterogeneity of the surface and the exponential distribution of sites and their energies [14]. The linear form of Freundlich equation (Eq. (7)) can be expressed as follows:

$$\log q_e = \frac{1}{n} \log C_e + \log K_f \quad (7)$$

$K_f$  (L/g) and  $n$  (–) are the characteristic constants of the system. The magnitude of dimensionless exponent  $n$  is related to the intensity of biosorption, where a value of  $n > 1$  represents favorable adsorption [16,27]. In this work, when plotting  $\log q_e$  vs.  $\log C_e$ , straight lines were obtained with  $R^2 \geq 0.96$ . The obtained exponent  $n$  (Tables 4 and 5) indicates the favorability of the adsorbent/adsorbate system at different temperatures (288, 303, and 318 K) onto heterogeneous surface of RS and SB sorbents, which implies stronger interaction between adsorbent and PAHs.

Temkin isotherm assumes that the heat of adsorption of all the molecules in a layer decreases linearly with the surface coverage of the adsorbent due to sorbate/adsorbate interactions. This adsorption is characterized by uniform distribution of binding energies [14,28]. The linear form of the Temkin isotherm equation (Eq. (8)) can be expressed as follows:

$$q_e = B \ln K_t + B \ln C_e \quad (8)$$

where  $B = RT/b$ ,  $T$  is the absolute temperature in K,  $R$  is the universal gas constant (8.314 J/K mol),  $K_t$  is the equilibrium binding constant. By plotting  $q_e$  vs.  $\ln C_e$ , straight lines were obtained with  $R^2 \geq 0.97$ .

The data obtained from the adsorption isotherms experiments listed in Tables 4 and 5 appeared to be well represented by all theoretical models tested. But Langmuir model expressed the highest  $R^2$  and lowest

$\Delta q_e\%$ , indicating that it gives the best fit and more accurately describes the sorption of the studied PAHs on the spent waste biomass of RS and SB. Furthermore, the Langmuir isotherm best fits the experimental data for lower values of  $C_e$ , indicating that initially the adsorption process occurred as a monolayer phenomenon. However, this does not persist under higher concentration ranges, where the adsorption seemed to be a multilayer process (Fig. 2). This gives a possibility of monolayer and hetero-layer PAHs molecules formation on the adsorbent surface. The spent waste RS and SB used in this study are composed of  $\approx 15$ –18% hemicellulose, 17–21% cellulose, 7–8% lignin, and the rest are ashes containing silicates and other minor and trace elements [29]. The presence of active functional groups with different intensities and nonuniform distribution may cause differences in the energy level of the active sites available on the RS and SB surfaces, which affect their biosorption capacity to form hetero-layer PAHs molecules coverage with robust support from strong chemical bonding and monolayer coverage due to electrostatic forces.

The intensity of adsorption constant  $K_L$ ,  $K_f$ , and  $K_t$  appear to be significantly higher for the PAH–SB system than PAH–RS system, which indicates greater affinity and better effectiveness for the three PAHs molecules onto SB biosorbent and confirming the importance of hydrophobicity of the RS and SB biosorbent surface in adsorbing the three PAHs. Within all the studied range of temperatures 288–318 K, the maximum sorption capacity ( $q_{max}$ , mg/g), the intensity of adsorption constant  $K_L$ ,  $K_f$ , and  $K_t$  calculated values of Nap, Ant, and Pyr adsorption system onto SB and RS increased by increasing the temperature of the wastewater solution (Tables 4 and 5) indicated easy uptake of studied pollutants from the authentic wastewater solution with an endothermic reaction. This is due to increase in the number of PAHs molecules acquiring energy that leads to increase the diffusion rate of the adsorbate molecules across the external boundary layer and in the internal pores of the adsorbent particles [30,31]. Furthermore, the maximum sorption capacity ( $q_{max}$ , mg/g),  $K_L$ , and  $K_f$  for PAHs uptake ranked in the following decreasing order; Nap > Ant > PYR onto either RS or SB that agrees well with active site pore filling phenomenon. The higher  $b$  values greater than 8 J/mol for the PAHs adsorption onto SB and RS adsorbents indicates strong interaction between the three PAHs species and SB and RS surface and implies the presence of chemisorption interaction of PAHs onto the adsorbent [14,32].

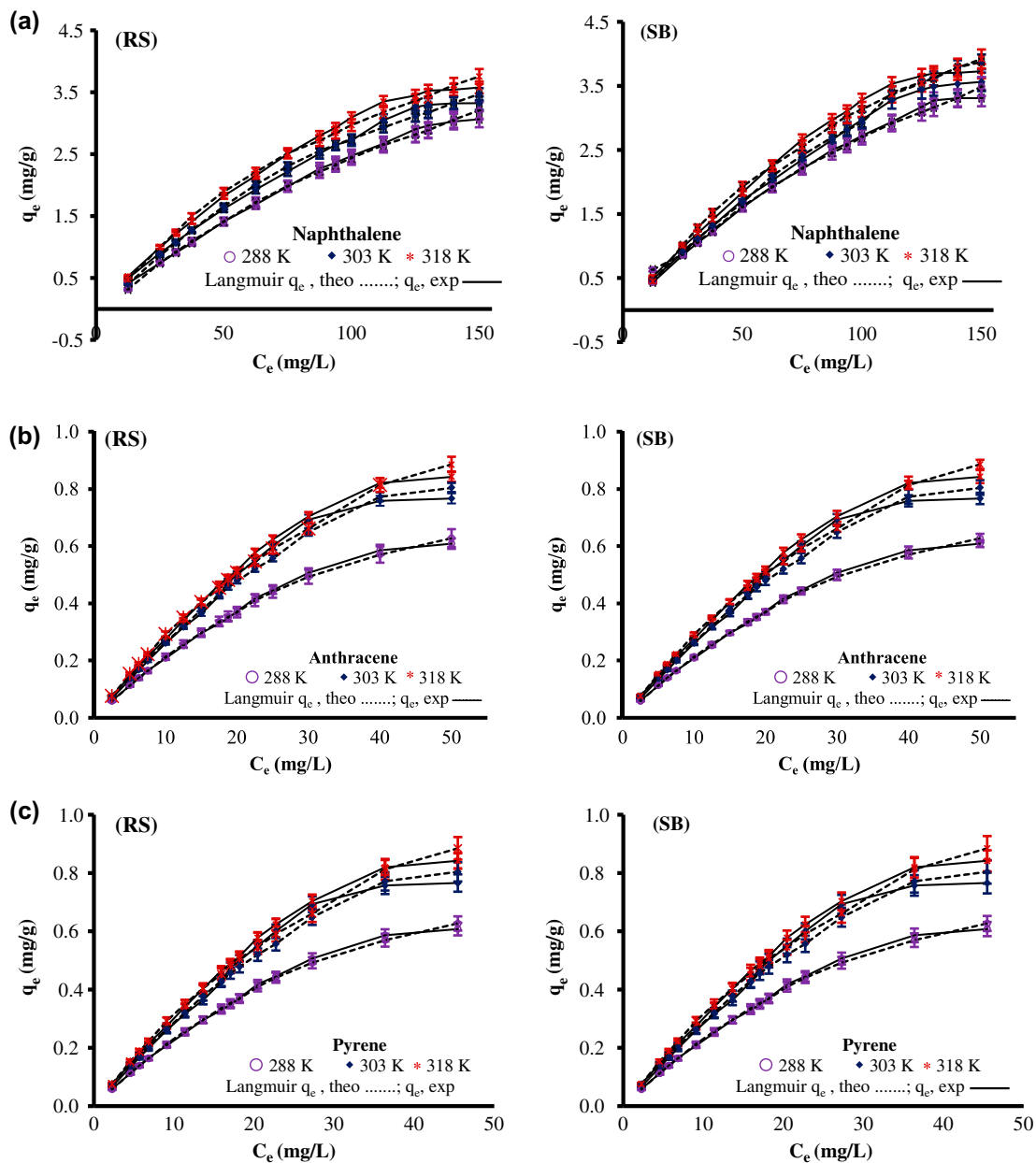


Fig. 2. Biosorption isotherm at different temperatures for (a) naphthalene, (b) anthracene, and (c) pyrene onto spent waste biomass of SB and RS.

### 3.4. Thermodynamic analyses

Thermodynamic parameters are calculated to understand the inherent energetic changes involved during the sorption process. The values of thermodynamic parameters of free energy of sorption  $\Delta G$  (kJ/mol), standard enthalpy  $\Delta H$  (kJ/mol), and standard entropy changes  $\Delta S$  (kJ/mol K) were calculated from Clausius–Clapeyron equations (Eqs. (9)–(11)):

$$\Delta G = -RT \ln K_L \quad (9)$$

$$\ln K_L = -\frac{\Delta G}{RT} = \frac{\Delta S}{R} - \frac{\Delta H}{RT} \quad (10)$$

$$\Delta G = \Delta H - T\Delta S \quad (11)$$

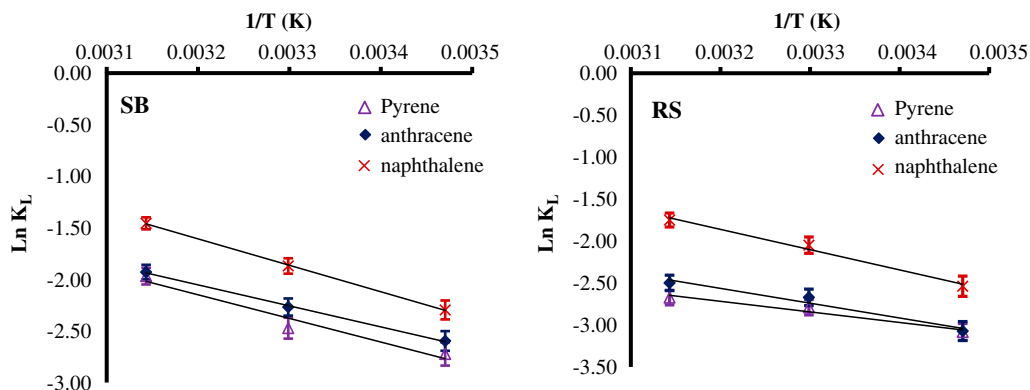


Fig. 3. Clausius–Clapeyron plots for adsorption of naphthalene, anthracene, and pyrene onto spent waste biomass of RS and SB.

Table 6

Thermodynamics parameters for biosorption of PAHs onto spent waste biomass RS and SB

PAHs	Temperature (K)	$\Delta G$ (kJ/mol)		$\Delta H$ (kJ/mol)		$\Delta S$ (J/mol K)	
		RS	SB	RS	SB	RS	SB
Naphthalene	288	6.08	5.50	20.10	21.32	48.9	54.9
	303	5.16	4.71				
	318	4.63	3.85				
Anthracene	288	7.36	6.22	14.66	16.94	25.6	37.1
	303	6.73	5.72				
	318	6.61	5.10				
Pyrene	288	7.39	6.52	10.48	19.07	10.9	43.2
	303	7.06	6.23				
	318	7.05	5.21				

Hence, a plot of  $\ln K_L$  vs.  $1/T$  yields a line with a slope  $= -\Delta H/R$  from which  $-\Delta H$  can be calculated (Fig. 3). From the data listed in Table 6, it can be concluded that the positive values of  $\Delta G$  imply the thermodynamic feasibility and nonspontaneous nature of three PAHs biosorption onto RS and SB. The  $\Delta G$  decreased with increase in temperature, indicating that temperatures play a positive role in the biosorption, and the adsorption mechanism associated with the removal of PAH onto RS and SB involves a temperature-dependent process (Fig. 2). The positive value of  $\Delta S$  reflects the good affinity of PAHs towards RS and SB and suggests the increase in randomness at the solid–solution interface during the sorption of PAHs molecules onto the biomass due to the dissolution of the adsorbing species, changes in the pores size of the adsorbents, and enhanced rate of intraparticle diffusion. The positive value of  $\Delta H$  indicates chemical adsorption, confirms the endothermic nature of the biosorption process which is an indication of the existence of a strong interaction between biomass and

PAHs molecules [14], and suggests some structural changes in adsorbate and adsorbent. By comparing the  $\Delta H$  and  $\Delta S$  values for the three PAHs on either RS or SB (Table 6), it was clearly observed that  $\Delta H$  and  $\Delta S$  for biosorption process onto SB is higher than onto RS. This indicated that the adsorption bonds between PAHs and RS adsorbent are weaker than those between PAHs and SB which confirm the higher affinity of PAHs molecules towards SB than RS. This agrees well with the experimental obtained results.

#### 4. Conclusions

In the view of the ubiquity, environmental compatibility, and cost-effectiveness, spent waste biomass of RS and SB as waste byproducts for bioethanol production process proved to be a favorable biosorbent for PAHs pollutants from PRWW with high sorption capacity of about 3.61–3.35 mg/g for 150 mg/L naphthalene, 1.01–0.77 mg/g for 50 mg/L anthracene, and 0.86–0.73 mg/g for 50 mg/L pyrene onto SB and RS,

respectively. The pseudo-first-order adsorption kinetic model best represented the adsorption kinetics data of naphthalene. The results of anthracene and pyrene appeared to be better adjusted to the kinetic model of pseudo-second order. The rapid observed kinetics of biosorption of PAHs molecules onto RS and SB have significant practical importance, as it will facilitate smaller reactor volumes ensuring efficiency and economy. Thermodynamic analyses indicate that the biosorption of PAHs molecules onto RS and SB takes place by combination of physical and chemical adsorption.

The results will provide a better understanding of sorption mechanisms and thermodynamics of PAHs adsorption from authentic wastewater solutions onto spent waste biomass of RS and SB, which would help in the development of more efficient adsorbate/adsorbent suitable for real-world application. .

Further application of these biosorbents for treatment of a real PRWW effluent is undertaken now in Egyptian Petroleum Research Institute.

## References

- [1] N.J. Aquilina, J.M. Delgado-Saborit, C. Meddings, S. Baker, R.M. Harrison, P. Jacob, M. Wilson, L. Yu, M. Duan, N.L. Benowitz, Environmental and biological monitoring of exposures to PAHs and ETS in the general population, *Environ. Int.* 36 (2010) 763–771.
- [2] X. Chen, J. Yu, Z.H. Zhang, C. Lu, Study on structure and thermal stability properties of cellulose fibers from rice straw, *J. Carbohydr. Polym.* 85 (2011) 245–250.
- [3] R. Crisafully, M.A. Milhome, R.M. Cavalcante, E.R. Silveira, D.D. De Keukeleire, R.F. Nascimento, Removal of some polycyclic aromatic hydrocarbons from petrochemical wastewater using low-cost adsorbents of natural origin, *Bioresour. Technol.* 99 (2008) 4515–4519.
- [4] D.T. Sponza, R. Oztekin, Destruction of some more and less hydrophobic PAHs and their toxicities in a petrochemical industry wastewater with sonication in Turkey, *Bioresour. Technol.* 101 (2010) 8639–8648.
- [5] Z. Aksu, J. Yener, A comparative adsorption/biosorption study of mono-chlorinated phenols onto various sorbents, *Waste Manage.* 21 (2001) 695–702.
- [6] Y. Li, B. Chen, L. Zhu, Enhanced sorption of polycyclic aromatic hydrocarbons from aqueous solution by modified pine bark, *Bioresour. Technol.* 101 (2010) 7307–7313.
- [7] L. Huang, T.B. Boving, B. Xing, Sorption of PAHs by aspen wood fibers as affected by chemical alterations, *Environ. Sci. Technol.* 40 (2006) 3279–3284.
- [8] S. Rodriguez-cruz, M.S. Andrades, M. Sanchez-camazano, M.J. Sanchez-martin, Relationship between the adsorption capacity of pesticides by wood residues and the properties of woods and pesticides, *Environ. Sci. Technol.* 41 (2007) 3613–3619.
- [9] A. Altınışık, E. Gür, Y. Seki, A natural sorbent, *Luffa cylindrica* for the removal of a model basic dye, *J. Hazard. Mater.* 179 (2010) 658–664.
- [10] D. Park, Y. Yun, J.M. Park, The past, present, and future trends of biosorption, *Biotechnol. Bioprocess Eng.* 15 (2010) 86–102.
- [11] M. Yuan, S. Tong, S. Zhao, C.Q. Jia, Adsorption of polycyclic aromatic hydrocarbons from water using petroleum coke-derived porous carbon, *J. Hazard. Mater.* 181(1–3) (2010) 1115–1120.
- [12] S.E. Agarry, M.O. Aremu, Batch equilibrium and kinetic studies of simultaneous adsorption and biodegradation of naphthalene by orange peels immobilized *Pseudomonas aeruginosa* NCIB 950, *J. Bioremed. Biodegrad.* 3(2) (2012) 138–150.
- [13] Sh.A. Younis, N.Sh. El-Gendy, W.I. El-Azab, Y.M. Moustafa, A.I. Hashem, The biosorption of phenol from petroleum refinery wastewater using spent waste biomass, *Energy Sources Part A* (2013) (Accepted in press).
- [14] J.Y. Farah, N.Sh. El-Gendy, Performance, kinetics and equilibrium in biosorption of anionic dye Acid Red 14 by the waste biomass of *Saccharomyces cerevisiae* as a low-cost biosorbent, *Turkish J. Eng. Environ. Sci.* 37 (2013) 146–161.
- [15] V.S. Mane, I. Deo Mall, V.C. Srivastava, Kinetic and equilibrium isotherm studies for the adsorption removal of Brilliant Green dye from aqueous solutions by rice husk ash, *J. Environ. Manage.* 84 (2007) 390–400.
- [16] M.N. Amin, A.I. Mustafa, M.I. Khalil, M. Rahman, I. Nahid, Adsorption of phenol onto rice straw biowaste for water purification, *Clean Technol. Environ. Policy* 14 (2012) 837–844.
- [17] A.A. MacKay, P.M. Gschwend, Sorption of monoaromatic hydrocarbons to wood, *Environ. Sci. Technol.* 34 (2000) 839–845.
- [18] K. Yang, X. Wang, L. Zhu, B. Xing, Competitive sorption of pyrene, phenanthrene, and naphthalene on multiwalled carbon nanotubes, *Environ. Sci. Technol.* 40(18) (2006) 5804–5810.
- [19] C.B. Vidal, A.L. Barros, C.P. Moura, A.C.A. de Lima, F.S. Dias, L.C.G. Vasconcellos, P.B.A. Fechine, R.F. Nascimento, Adsorption of polycyclic aromatic hydrocarbons from aqueous solutions by modified periodic mesoporous organosilica. *J. Colloid Interface Sci.* 357 (2011) 466–473.
- [20] Y.S. Ho, G. McKay, Pseudo-second-order model for sorption processes, *Process Biochem.* 34 (1999) 451–465.
- [21] M.R. Pérez-Gregorio, M.S. García-Falcón, E. Martínez-Carballo, J. Simal-Gándara, Removal of polycyclic aromatic hydrocarbons from organic solvents by ashes wastes, *J. Hazard. Mater.* 178 (2010) 273–281.
- [22] Y.S. Ho, Removal of copper ions from aqueous solution by tree fern, *Water Res.* 37(10) (2003) 2323–2330.
- [23] I. Langmuir, The constitution and fundamental properties of solids and liquids. Part I. solids, *J. Am. Chem. Soc.* 38(11) (1916) 2221–2295.
- [24] H.M.F. Freundlich, Über die adsorption in lösungen (Over the adsorption in solution), *Zeitschrift für Physikalische Chemie (J. Phys. Chem.)* 57 (1906) 385–470.

- [25] M.J. Temkin, V. Pyzhev, Kinetics of ammonia synthesis on promoted iron catalysis, *Acta Physicochim. URSS*. 12 (1940) 327–356.
- [26] V. Srihari, A. Das, Adsorption of phenol from aqueous media by an agro-waste (*Hemidesmus indicus*) based activated carbon, *Appl. Ecol. Environ. Res. (AEER)* 7 (1) (2009) 13–23.
- [27] H. Zhang, A. Li, J. Sun, P. Li, Adsorption of amphoteric aromatic compounds by hyper-cross-linked resins with amino groups and sulfonic groups, *Chem. Eng. J.* 217 (2013) 354–362.
- [28] Y. Liu, Y.J. Liu, Biosorption isotherms, kinetics and thermodynamics, *Sep. Purif. Technol.* 61 (2008) 229–242.
- [29] M.A. Abo-State, A.M.A. Ragab, N.Sh. EL-Gendy, L.A. Farahat, H.R. Madian, Effect of different pretreatments on Egyptian sugar-cane bagasse saccharification and bioethanol production, *Egypt. J. Petrol.* 22(1) (2013) 161–167.
- [30] M. Ajmal, R.A.K. Rao, R. Ahmad, J. Ahmad, Adsorption studies on *Citrus reticulata* (fruit peel of orange): removal and recovery of Ni(II) from electroplating wastewater, *J. Hazard. Mater. B* 79 (2000) 117–131.
- [31] V.K. Gupta, I. Ali, A. Suhas, D. Mohan, Equilibrium uptake and sorption dynamics for the removal of a basic dye (basic red) using low-cost adsorbents, *J. Colloid Interface Sci.* 265 (2003) 257–264.
- [32] H.K. Boparai, M. Joseph, D.M. O'Carroll, Kinetics and thermodynamics of cadmium ion removal by adsorption onto nano zerovalent iron particles, *J. Hazard. Mater.* 186 (2011) 458–465.